



Universiteit
Leiden
The Netherlands

Gangliosides and anti-ganglioside antibodies in neuromuscular synaptic function

Zitman, F.M.P.

Citation

Zitman, F. M. P. (2010, January 20). *Gangliosides and anti-ganglioside antibodies in neuromuscular synaptic function*. Retrieved from <https://hdl.handle.net/1887/14568>

Version: Corrected Publisher's Version

License: [Licence agreement concerning inclusion of doctoral thesis in the Institutional Repository of the University of Leiden](#)

Downloaded from: <https://hdl.handle.net/1887/14568>

Note: To cite this publication please use the final published version (if applicable).

CHAPTER 3.2

Eculizumab prevents anti-ganglioside antibody-mediated neuropathy in a murine model

**Susan K. Halstead^{a,*}, Femke M.P. Zitman^{b,c,*},
Peter D. Humphreys^a, Kay N. Greenshields^a, Jan J.
Verschuuren^b, Bart C. Jacobs^d, Russell P. Rother^e,
Jaap J. Plomp^{b,c}, and Hugh J. Willison^a**

^aDivision of Clinical Neurosciences, Glasgow Biomedical Research Centre,
University of Glasgow, Glasgow G12 8TA, UK.

Departments of ^bNeurology and ^cMolecular Cell Biology – Group
Neurophysiology, Leiden University Medical Centre, PO Box 9600, NL-2300
RC Leiden, The Netherlands.

^dDepartments of Neurology and Immunology, Erasmus MC, 3015 CE,
Rotterdam, The Netherlands.

^eAlexion Pharmaceuticals, Cheshire, CT 06410, USA.

* These authors contributed equally to this work

Published in Brain 131 (2008), 1197 - 1208

Abstract

Anti-GQ1b ganglioside antibodies are the serological hallmark of the Miller Fisher syndrome (MFS) variant of the paralytic neuropathy, Guillain-Barré syndrome, and believed to be the principal pathogenic mediators of the disease. In support of this, we previously showed in an *in vitro* mouse model of MFS that anti-GQ1b antibodies were able to bind and disrupt presynaptic motor nerve terminals at the neuromuscular junction (NMJ) as one of their target sites, thereby causing muscle paralysis. This injury only occurred through activation of complement, culminating in the formation and deposition of membrane attack complex (MAC, C5b-9) in nerve membranes. Since this step is crucial to the neuropathic process and an important convergence point for antibody and complement mediated membrane injury in general, it forms an attractive pharmacotherapeutic target. Here, we assessed the efficacy of the humanized monoclonal antibody eculizumab, which blocks the formation of human C5a and C5b-9, in preventing the immune-mediated motor neuropathy exemplified in this model. Eculizumab completely prevented electrophysiological and structural lesions at anti-GQ1b antibody pre-incubated NMJs *in vitro* when using normal human serum as a complement source. In a novel *in vivo* mouse model of MFS generated through intraperitoneal injection of anti-GQ1b antibody and normal human serum, mice developed respiratory paralysis due to transmission block at diaphragm NMJs, resulting from anti-GQ1b antibody binding and complement activation. Intravenous injection of eculizumab effectively prevented respiratory paralysis and associated functional and morphological hallmarks of terminal motor neuropathy. We show that eculizumab protects against complement-mediated damage in murine MFS, providing the rationale for undertaking clinical trials in MFS and other antibody-mediated neuropathies in which complement activation is believed to be involved.

Acknowledgements

This work was supported by grants from the Wellcome Trust (#077041/Z/05/Z, to HJW) and the Prinses Beatrix Fonds (#MAR04-0213, to JJP).

Introduction

Miller Fisher syndrome (MFS) is characterized by the triad of ataxia, areflexia and ophthalmoplegia (Fisher, 1956) and is a clinical variant of the post-infectious paralytic neuropathy, Guillain-Barré syndrome (GBS) (Hughes and Cornblath, 2005). MFS is associated with anti-GQ1b ganglioside antibodies that are considered to be the predominant pathogenic factor and may arise through molecular mimicry during a preceding infection with *Campylobacter jejuni* or other microbes bearing GQ1b mimics in their lipooligosaccharide (Goodyear et al., 1999; Willison and O'Hanlon, 1999; Yuki, 2001; Bowes et al., 2002). Gangliosides are a family of sialylated glycosphingolipids that are enriched in neuronal cell membranes (Ledeen, 1985). Ophthalmoplegia in MFS is thought to be related to the relatively high GQ1b ganglioside level in oculomotor nerves, forming a preferential antigenic target for anti-GQ1b antibodies (Chiba et al., 1993). Furthermore, anti-GQ1b antibody binding to the presynaptic motor nerve terminal compartment of the neuromuscular junction (NMJ), causing synaptic transmission block, has been proposed by us and others from animal studies (Roberts et al., 1994; Buchwald et al., 1995; Plomp et al., 1999). This idea was based on data that 1) botulism, an established NMJ disorder, is an important differential diagnosis for MFS, 2) cholinergic synapses are highly enriched in gangliosides (Schwarz and Futerman, 1996) and 3) NMJs are easily accessible by antibodies because there is no blood-nerve barrier. A number of case studies have since supplied clinical electrophysiological indications for NMJ dysfunction in MFS (Uncini and Lugaesi, 1999; Wirguin et al., 2002; Sartucci et al., 2005; Lange et al., 2006; Lo et al., 2006).

We have developed an *in vitro* experimental mouse model for MFS in which NMJs of the diaphragm-phrenic nerve preparation are exposed to mouse or human (monoclonal) anti-GQ1b antibodies or anti-GQ1b positive patient sera. The model has been extensively characterized in electrophysiological, morphological and functional studies (Goodyear et al., 1999; Plomp et al., 1999; Bullens et al., 2000; O'Hanlon et al., 2001; Jacobs et al., 2002; Halstead et al., 2004). These studies demonstrate that both human and mouse anti-GQ1b polyclonal antisera and monoclonal antibodies bind to the presynaptic motor nerve ending and activate the complement cascade, culminating in the formation of membrane attack complex (MAC, C5b-9). This pore-forming complex damages the presynaptic membrane, causing uncontrolled neurotransmitter release, ultrastructural destruction of the nerve terminal, and finally, blockade of neuromuscular transmission with resultant paralysis.

Tissue-bound antibody of the appropriate class fixes complement and experimental neuropathological effects in our MFS model are strictly dependent on complement activation (Plomp et al., 1999; Bullens et al., 2000; Halstead et al., 2004). Furthermore, there is evidence of complement involvement in variants of GBS (Sanders et al., 1986; Koski et al., 1987; Hartung et al., 1987; Hafer-Macko et al., 1996a). In view of the above, the complement system is an attractive target for pharmacotherapeutic intervention in MFS, and has led us to examine inhibitors of complement activation as potential therapies for the disease in humans, and by inference, also for pathophysiologically similar forms of GBS and other autoimmune neuropathies, including chronic inflammatory demyelinating polyneuropathy and multifocal motor neuropathy (Halstead et al., 2005a). Eculizumab (Soliris, Alexion Pharmaceuticals) is a humanized monoclonal antibody (mAb) that specifically binds to and blocks the cleavage of human complement component C5, thereby preventing

the formation of the proinflammatory and cell lytic molecules C5a and C5b (Thomas et al., 1996). Targeted blockade of complement at C5 preserves the earlier immunoprotective effects of complement activation (e.g. C3b opsonisation and phagocytosis). In addition to protecting against antibody mediated effects, complement inhibitors also have the potential to protect against secondary events such as those occurring in Wallerian degeneration (Ramaglia et al., 2007). Eculizumab has recently been approved to treat paroxysmal nocturnal haemoglobinuria, a genetic disorder with complement-mediated haemolysis as the primary clinical manifestation (Hillmen et al., 2006).

Here, we investigated the possible benefit of eculizumab in immune-mediated neuropathy by assessing its effects in the existing *in vitro* model for MFS and in a newly generated *in vivo* mouse model with paralytic symptoms. Despite extensive *in vitro* data, characterization of an anti-GQ1b antibody mediated clinical phenotype in active or passive immunisation models in the living mouse has not been achieved to date. Here we have used plethysmography to quantify respiratory function in living mice passively immunized with anti-GQ1b antibody and human complement through intraperitoneal injection and demonstrate the rapid development of a severe respiratory phenotype. Eculizumab completely prevented the presynaptic electrophysiological dysfunction and structural damage at *in vitro* NMJs that had been pre-incubated with anti-GQ1b mAb and efficiently prevented *in vivo* respiratory paralysis in the newly developed *in vivo* MFS mouse model.

Methods

Mice

Male Balb/c mice (3-6 weeks old, 10-25 g) were obtained from Harlan (UK or NL). In some muscle contraction experiments (see below) male and female GM2synthase *null*-mutant mice (Bullens et al., 2002) were used at 12-22 weeks of age (19-37 g). All animal experiments were carried out in accordance to UK Home Office guidelines (UK PPL60/3096), Dutch law and Glasgow and Leiden University guidelines.

Monoclonal antibodies and normal human serum

The IgM anti-GQ1b ganglioside mAb, CGM3 was derived from mice inoculated with a GT1a-bearing *C. jejuni* lipooligosaccharide (Goodyear et al., 1999). CGM3 reacts with gangliosides GQ1b, GD3 and GT1a that all share the terminal disialylgalactose structure. Previous *in vitro* studies have shown that CGM3 has similar ganglioside specificity and induces identical complement-dependent pathogenic effects as human MFS sera (Goodyear et al., 1999; Plomp et al., 1999; Bullens et al., 2000; Jacobs et al., 2002; Jacobs et al., 2003). The advantage of using a mAb for these studies is that, unlike human sera, it is a quantitatively unlimited and homogeneous resource that can be fully quantified and characterized and prepared as a stock solution for long-term use during the course of the experiments. CGM3 concentration was measured using quantitative ELISA (Bethyl Laboratories). Normal human serum (NHS) was taken from a single donor stock that had been freshly frozen and stored in multiple aliquots at -70 °C to preserve complement activity. Prior to experimental use, CGM3 and NHS were dialyzed for 24 h at 4 °C against Ringer's solution (116mM NaCl, 4.5mM KCl, 1mM MgCl₂, 2mM CaCl₂, 1mM NaH₂PO₄, 23mM NaHCO₃, 11mM glucose, pH 7.4), pre-gassed with 95% O₂ /5% CO₂. The humanized anti-human C5 mAb eculizumab

and a non-specific isotype-matched control mAb ALXN3300 were obtained from Alexion Pharmaceuticals and stored at 4 °C. Eculizumab binds plasma C5 only and thereby prevents its cleavage into C5a and C5b in the liquid-phase, but does not bind to membrane bound C5b as part of the MAC complex. The anti-C5 antibody is therefore not deposited in the tissue. Eculizumab is also monospecific for human C5, and does not bind to C5 from other species, including the mouse. Thus in this model, eculizumab is only capable of neutralizing the heterologous C5 in the human serum added as a final step in the *in vitro* exposure and passive immunization paradigms.

***In vitro* MFS model**

The *in vitro* model for MFS using CGM3 and NHS has been described before (Goodyear et al., 1999; O'Hanlon et al., 2001). In short, mouse hemi-diaphragms with phrenic nerve attached (or triangularis sterni muscle in some cases for illustrative NMJ immunohistology) were dissected and mounted in Ringer's medium at room temperature (20-22 °C). Untreated small control sections were removed from each muscle preparation prior to any incubation and snap frozen on dry ice for subsequent baseline immunohistological analysis. Muscles were incubated with CGM3 (50 µg/ml) for 2-2.5 h at 32 °C, then for 30 min at 4 °C and then equilibrated for 10 min at room temperature, rinsed in Ringer's medium and subsequently exposed to 33 or 40% NHS in Ringer's medium for 1 h at room temperature. Eculizumab (100 µg/ml) or the control mAb (100 µg/ml) was mixed with NHS 10 min prior to the incubation of the muscle preparation. *In vitro* electrophysiological measurements at the NMJ (see below) and scoring of muscle fibre twitching, a hallmark of uncontrolled transmitter release at NMJs in this model (O'Hanlon et al., 2001; Jacobs et al., 2002), were performed before and after CGM3 incubation, and during the 1 h NHS incubation. Muscle strips were frozen on dry ice and stored at -20 °C, both before and after incubation with NHS. NMJs and terminal motor axons were assessed for levels of IgM, C3c, MAC, neurofilament (NF) and for perisynaptic Schwann cell (pSC) viability (see below).

***In vivo* MFS model**

Balb/c mice (3-4 weeks old, 10-15 g) were injected intraperitoneally with 1.5 mg CGM3, followed 16 h later by an intraperitoneal injection of 0.5 ml 100% NHS. Mice were observed for a further 4-6 h and analyzed with whole-body plethysmography (see below) and grip strength testing as described before (Kaja et al., 2007a). The mice were then killed by CO₂ asphyxiation and hemi-diaphragm muscle tissue was dissected and analyzed in electrophysiological and muscle contraction experiments (see below) or further processed for immunohistological analyses (see below). The effect of eculizumab on the *in vivo* symptoms and the subsequently analyzed electrophysiological, functional and histological lesions was tested in this model by injecting 200 µg eculizumab or control mAb in the tail vein, shortly before intraperitoneal NHS injection. Initial dose-range finding experiments (data not shown) indicated that eculizumab at doses of >50 µg/mouse protected against neuropathy.

Plethysmography

Non-invasive whole-body plethysmography (EMMS) was employed to demonstrate changes in breathing parameters in *in vivo* experiments. Baseline data was collected prior to onset of experiment. Mice were injected with CGM3 followed by NHS with eculizumab or control mAb 16 h later (protocol as above) and monitored continuously

for 6 h. Flow derived parameters of breath frequency and tidal volume were collected from 25 accepted breaths and averaged over 1 h periods.

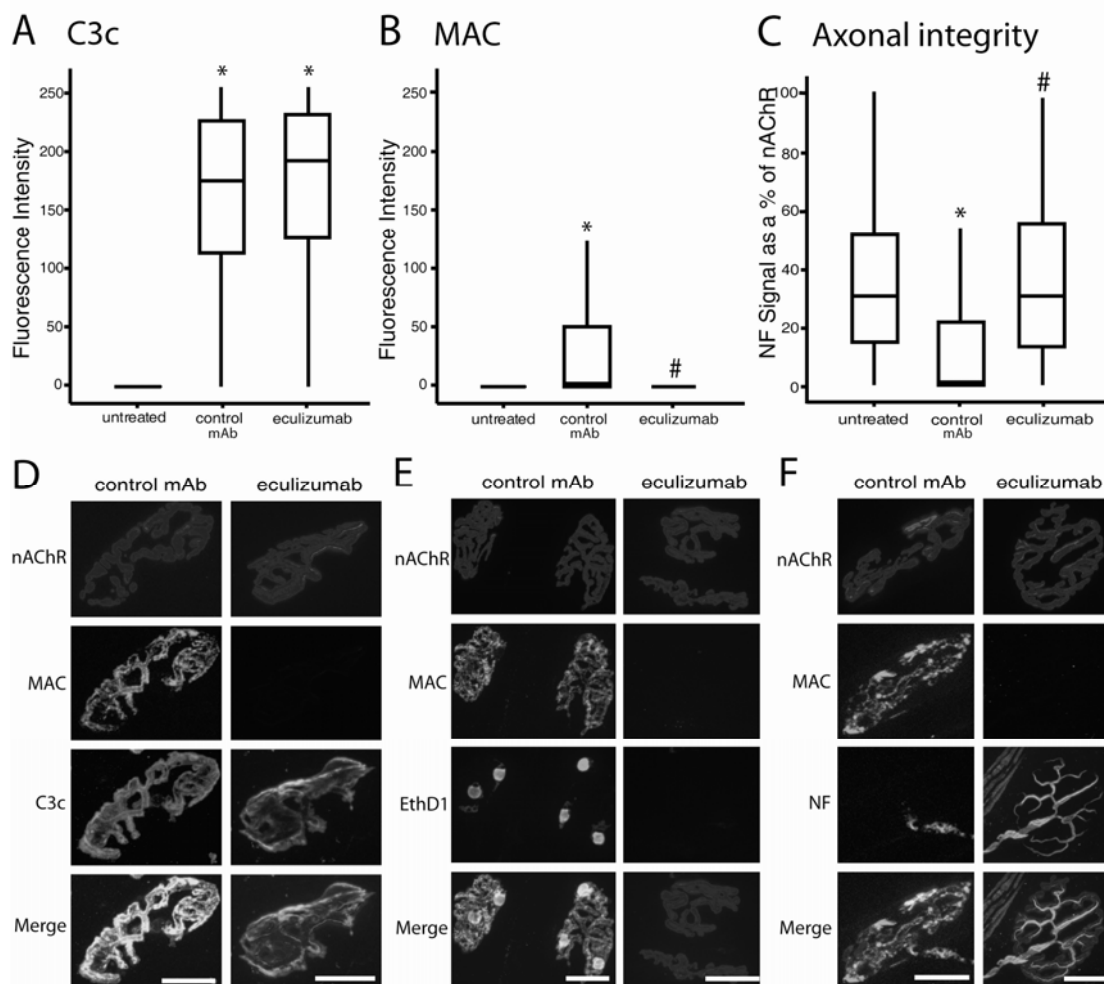


Figure 3.8. Immunohistological demonstration of the protective effect of eculizumab against MAC deposition and terminal motor axonopathy at NMJs in the *in vitro* MFS model. Mouse hemi-diaphragm preparations were pre-incubated with anti-GQ1b ganglioside mAb CGM3 (50 $\mu\text{g/ml}$) and subsequently treated with 40% normal human serum (NHS) with either added eculizumab (anti-human C5 neutralizing mAb; 100 $\mu\text{g/ml}$) or non-specific isotype-matched control mAb (100 $\mu\text{g/ml}$), and compared with untreated tissue. **A.** Tissues treated with NHS/eculizumab showed intense C3c staining at NMJs, similar to that of NHS/control mAb-treated tissues ($p=0.12$). **B.** Membrane attack complex (MAC) staining was not observed (intensity comparable to baseline, $p=0.92$), indicating complete inhibition of terminal complement. **C.** Axonal integrity was preserved, as assessed by presence of neurofilament (NF) signal, comparable to baseline in untreated controls ($p=0.80$). **D-F.** Illustrative immunofluorescent images of NMJs in whole-mount muscle demonstrating the protective effect of eculizumab against MAC deposition (**D**), perisynaptic Schwann cell damage (stained with ethidium homodimer-1; EthD1; **E**) and terminal motor axonal damage (**F**), as compared to NHS/control mAb treatment. Postsynaptic nicotinic acetylcholine receptor (nAChR) staining was used to delineate the NMJ. Intermediate complement protein C3c (**D**) remains abundantly deposited at NMJs.

* $p<0.01$, different from untreated; # $p<0.01$, different from control mAb-treated; scale bar: 20 μm .

***In vitro* electrophysiological analysis of NMJs and visual scoring of muscle contractility**

Left and right hemi-diaphragms with their phrenic nerve attached were dissected and pinned out in a silicone rubber-lined dish in 1.5 ml Ringer's medium at room temperature. Intracellular recordings of miniature endplate potentials (MEPPs, the postsynaptic events arising from spontaneous release of single acetylcholine quanta from the presynaptic motor nerve terminal) were made at NMJs at 20-22 °C. Muscle fibres were impaled near the NMJ with a 10-20 M Ω glass micro-electrode filled with 3 M KCl, connected to a GeneClamp 500B amplifier (Axon Instruments/Molecular Devices) for amplifying and filtering (10 kHz low-pass) of the signal. Signals were digitized, stored and analyzed (off-line) using a Digidata 1322A interface, Clampex 9.2 and Clampfit 9.2 programs (all from Axon Instruments/ Molecular Devices), Mini Analysis 6.0 (Synaptosoft) and routines programmed in Matlab (The MathWorks Inc.).

The occurrence of spontaneous asynchronous fibre twitches that are induced by a high MEPP frequency resulting from CGM3/complement-mediated presynaptic damage (Plomp et al., 1999) was scored visually every 5 min (O'Hanlon et al., 2001). The tissue scored 0 for no activity, 1 for the twitching of <10 fibres, 2 for a small amount of twitching across the tissue, 3 for a moderate amount and 4 for an extensive amount. The average score during each measuring period was calculated. The final result of CGM3/complement-mediated presynaptic damage is a silencing of synaptic transmission at the NMJ. The number of "silent" NMJs (i.e. without detectable MEPPs and occurrence of phrenic nerve-stimulation evoked muscle action potentials) was expressed as percentage of the total number of NMJs sampled (8-41) in a muscle under each experimental condition.

Muscle contraction experiments

The protective efficacy of eculizumab on *in vitro* CGM3/NHS-induced loss of nerve stimulation-evoked contraction force of the hemi-diaphragm preparation was tested. We used diaphragm from GM2synthase *null*-mutant mice because earlier studies showed a somewhat higher sensitivity of muscle of this strain to CGM3/NHS-induced loss of contraction (Bullens et al., 2002). Left and right phrenic nerve-hemi-diaphragm preparations that had been pre-incubated with 200 μ g/ml CGM3 for 3 h at 32 °C were mounted in a silicone-rubber lined dish containing 2.25 ml Ringer's medium at room temperature (20-22 °C), continuously bubbled with 95% O₂ / 5% CO₂. The ribcage side of the muscle was thoroughly fixed to the bottom of the dish by multiple small pins and the central tendon was connected via a metal hook and a string to a force transducer that was connected to an amplifier and digitizing equipment, as described earlier (Kaja et al., 2007a). Supramaximal stimuli (usually ~10 V) of 100 μ s duration were delivered every 5 min for 3 s at 40 Hz from a Master-8 programmable stimulator (AMPI). Basic tension was adjusted with a vernier control to obtain maximal stimulated tetanic contraction force (usually about 10 g). Stability of the elicited contraction was monitored for 30-50 min. Subsequently, the medium was replaced by NHS (33%) to which eculizumab (3, 6, 9, 12, 25, 50 or 100 μ g/ml) had been added and admixed for ~10 min prior to addition and the effect was monitored for 100-200 min, under continuous gentle bubbling with 95% O₂ / 5% CO₂. In the control experiments without added eculizumab, 100 μ g/ml of the control mAb was added to the NHS. The amplitude of contractions was cursor-measured off-line in the Clampfit 9.0 program (Axon Instruments/Molecular devices), at 2 s after the start of the each nerve stimulation train.

Tetanic and twitch contraction forces were also measured upon *in vitro* nerve stimulation of left hemi-diaphragm muscles that were dissected from mice that had been subjected to the *in vivo* MFS protocol.

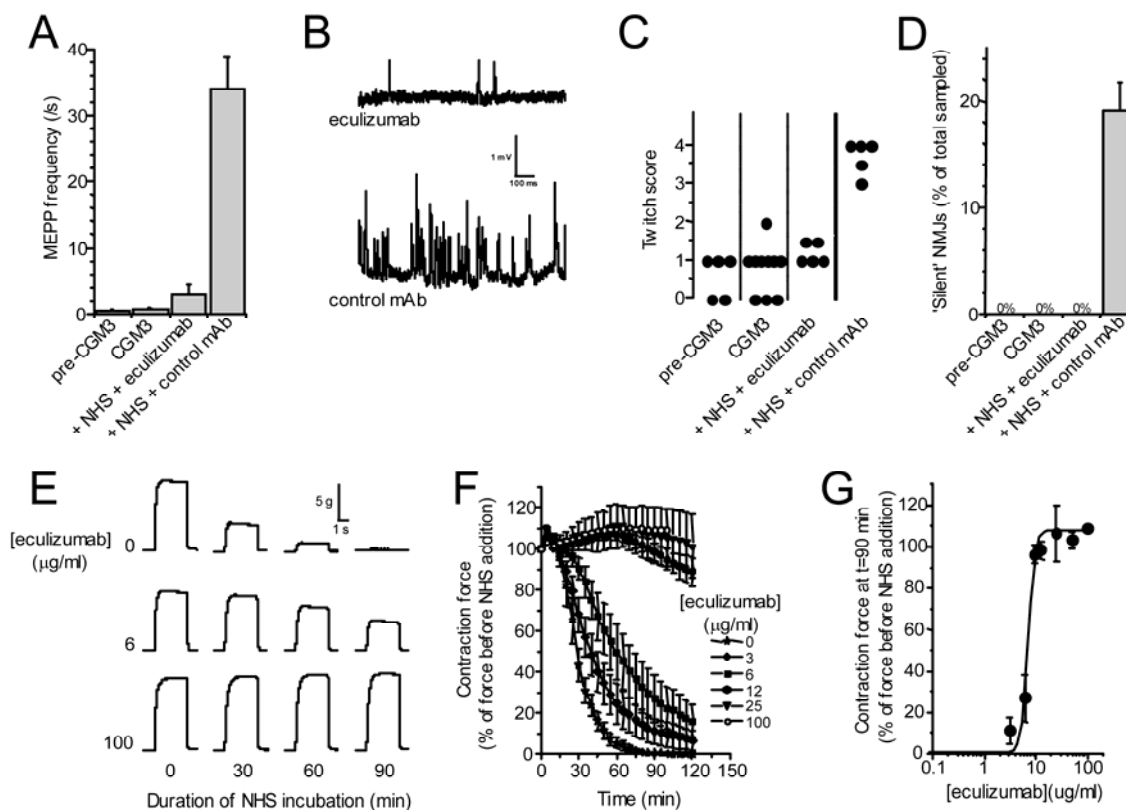


Figure 3.9. Eculizumab protects against electrophysiological and functional defects induced at NMJs in the *in vitro* MFS model. Mouse hemi-diaphragm preparations were pre-incubated with anti-GQ1b ganglioside mAb CGM3 (50 $\mu\text{g/ml}$) and subsequently treated with 40% normal human serum (NHS) with either added 100 $\mu\text{g/ml}$ eculizumab (anti-human C5 neutralizing mAb) or non-specific isotype-matched control mAb. **A.** Spontaneous unquantal acetylcholine release, measured as MEPP frequency, at the NMJ. Eculizumab prevented the induction of a high MEPP frequency by NHS at CGM3-incubated NMJs ($p < 0.001$, $n = 5$ muscles). **B.** Representative 1 s duration traces obtained during incubation with NHS, either with added eculizumab (upper trace) or control mAb (lower trace). **C.** Asynchronous twitching of muscle fibres induced by NHS was largely prevented by eculizumab ($p < 0.01$, $n = 5$ muscles). **D.** Eculizumab completely prevented the occurrence of “silent” NMJs (i.e. without detectable synaptic electrophysiological signals). **E-G.** Hemi-diaphragm muscle-nerve preparations were pre-incubated with 200 $\mu\text{g/ml}$ CGM3 and the protective effect of several concentrations eculizumab (0-100 $\mu\text{g/ml}$, $n = 2-5$ muscles per concentration) added to the NHS was observed in muscle contraction force recording experiments. **E.** Examples of the contraction profiles observed at 0, 30, 60 and 90 min after the start of the NHS incubation with either no eculizumab added or 6 or 100 $\mu\text{g/ml}$ added. Each contraction was elicited by supramaximal electric stimulation of the phrenic nerve for 3 s at 40 Hz. **F.** Development of the contraction loss during NHS incubation with the various concentrations eculizumab added. **G.** Concentration-effect relationship of eculizumab and the protection against loss of contraction after 90 min after the start of the NHS incubation. A Boltzmann sigmoidal curve is fitted through the data points, yielding an EC_{50} of 7.1 $\mu\text{g/ml}$. Error bars in panels **A**, **D**, **F** and **G** represent SEM.

Immunohistological analyses

Unfixed hemi-diaphragm sections were mounted in Lipshaw's M-1 mounting medium, and longitudinal cryostat sections (8-20 μm) were cut onto 3-aminopropyltriethoxysilane coated slides, air-dried, then stored at $-20\text{ }^{\circ}\text{C}$. To localize NMJs, TRITC and bodipy-labelled α -bungarotoxin (αBTx , diluted 1/750 to 1.3 $\mu\text{g}/\text{ml}$; Molecular Probes) were used. The intermediate complement component C3c was detected by incubation with FITC-labelled rabbit anti-C3c (1/300; Dako) for 1 h at $4\text{ }^{\circ}\text{C}$. MAC was detected using mouse anti-human C5b-9 (1/50; Dako) followed by FITC conjugated goat anti-mouse IgG (1/300), both for 1 h at $4\text{ }^{\circ}\text{C}$.

For NF staining, sections of unfixed tissue were pre-incubated for 1 h at $4\text{ }^{\circ}\text{C}$ with TRITC-conjugated αBTx , rinsed, immersed in ethanol at $-20\text{ }^{\circ}\text{C}$ for 20 min, then incubated overnight at room temperature with the rabbit polyclonal serum 1211 (1/750; reactive with phosphorylated NF; Affiniti Research Products Ltd.) followed by FITC conjugated goat anti-rabbit IgG (1/300; Southern Biotechnology Associates) for 3 h at $4\text{ }^{\circ}\text{C}$. All detection antibodies were diluted in phosphate-buffered saline (PBS).

pSC viability was assessed using ethidium homodimer-1 (EthD-1), a membrane impermeant dye that labels with red fluorescence the nucleic acids of membrane-permeabilized cells (Molecular Probes). In brief, nerve-muscle preparations were exposed to Ringer's containing 2 μM EthD-1. The tissue was incubated in the dark at room temperature for 1 h, rinsed in Ringer's solution and frozen for immunohistology. NMJs were identified in 15 μm cryostat sections by staining with bodipy conjugated αBTx (1.3 $\mu\text{g}/\text{ml}$), and the percentage of NMJ with EthD-1 positive nuclei at NMJs was calculated.

For illustrations, whole mount triangularis sterni muscles were incubated with CGM3 (50 $\mu\text{g}/\text{ml}$) and fluorochrome-conjugated αBTx (TRITC/FITC/Cy5) (2 $\mu\text{g}/\text{ml}$; 1:500), followed by NHS plus eculizumab or control mAb. Preparations were incubated with fluorescently conjugated αBTx and various combination of the following: mouse anti-C5b-9 (1:40; Dako), anti-C3c-FITC (1:200; Dako), or EthD-1 (2 μM) in Ringer's medium for 1 h at room temperature, rinsed in Ringer's medium, followed by fixation for 20 min in 4% formaldehyde in PBS. Unreactive aldehyde groups were quenched, by incubating with 0.1 M glycine for 10 min. The antibodies were then reapplied in PBS and agitated overnight at room temperature. For staining of intracellular antigens, muscle was fixed in 4% formaldehyde for 20 min followed by 10 min in 0.1M glycine and then incubated in a permeabilizing solution of 0.5% Triton-X100 in PBS for 30 min at RT, and either rabbit anti-S100 (1:150; Dako) or rabbit anti-NF (1:150; Chemicon) diluted in permeabilizing solution applied overnight at room temperature. Tissue was rinsed in PBS and where necessary incubated in the following fluorescently conjugated antibodies diluted 1:300; anti-rabbit IgG-FITC, anti-mouse IgG-FITC or -TRITC and agitated for 7h at room temperature in the dark. Tissue was rinsed in PBS and mounted in Citifluor mounting medium (Citifluor Products).

Image acquisition, quantitation and statistical analysis

Digital images were captured using both Zeiss Pascal confocal laser scanning microscope and Zeiss Axio Imager Z1 with ApoTome. Image-analysis measurements were made using Scion Image (Scion Corporation Frederick) image analysis software. For quantitative analysis of IgM, C3c, MAC and NF, three staining runs of each marker were performed on tissue from at least three individual hemi-diaphragms, and quantified as previously described (O'Hanlon et al., 2001). All studies were observer blinded. For immunohistological analysis of non-parametric data, statistical

comparisons were made using Mann-Whitney Test employing a 1% level of significance. For comparison of EthD-1 positive pSC at the NMJ, chi-squared test was used at 1% level of significance.

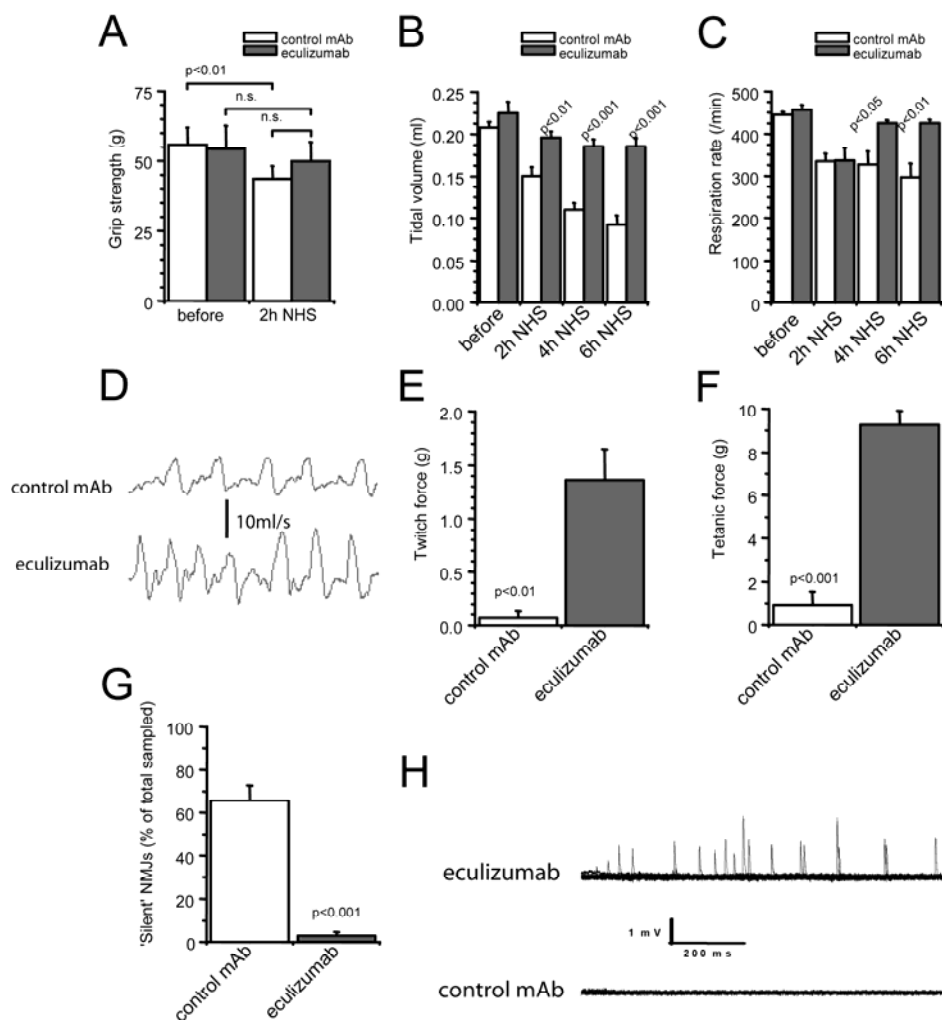


Figure 3.10. Respiratory paralysis in the *in vivo* MFS model is prevented by eculizumab due to inhibition of presynaptic block of neuromuscular transmission in the diaphragm. Mice ($n=6$) were intraperitoneally injected with 1.5 mg anti-GQ1b ganglioside mAb CGM3 and, 16 h later, with 0.5 ml 100% normal human serum (NHS) as complement source. A dose of 200 μ g eculizumab or control mAb was injected in the tail vein shortly before the NHS injection. **A.** Grip strength analysis at 2h post-NHS injection. Eculizumab prevented the loss of pulling force observed in the control mAb group ($p<0.01$). **B.** Average tidal volume and **C.** breathing rate measured with whole-body plethysmography before NHS injection and during the 2nd, 4th and 6th hour post-NHS injection. The development of breathing difficulty was prevented by eculizumab. **D.** Example 1 s traces of plethysmography flow rate obtained in eculizumab- and control mAb-treated mice. **E.** Twitch force and **F.** tetanic force elicited in the dissected diaphragm muscle by single and 40 Hz electrical nerve stimulation, respectively. Eculizumab completely prevented the severe paralysis observed in muscles from control mAb-treated mice ($p<0.01$). **G.** Eculizumab almost completely prevented the occurrence of “silent” NMJs (i.e. without detectable synaptic electrophysiological signals) in these mice ($p<0.001$). **H.** Thirty superimposed representative traces of 1 s duration obtained in NMJs of muscle from eculizumab-treated (upper traces) or control mAb-treated (lower traces) mice.

Error bars in the bar graph panels of this figure represent SEM.

n.s.: not statistically significant

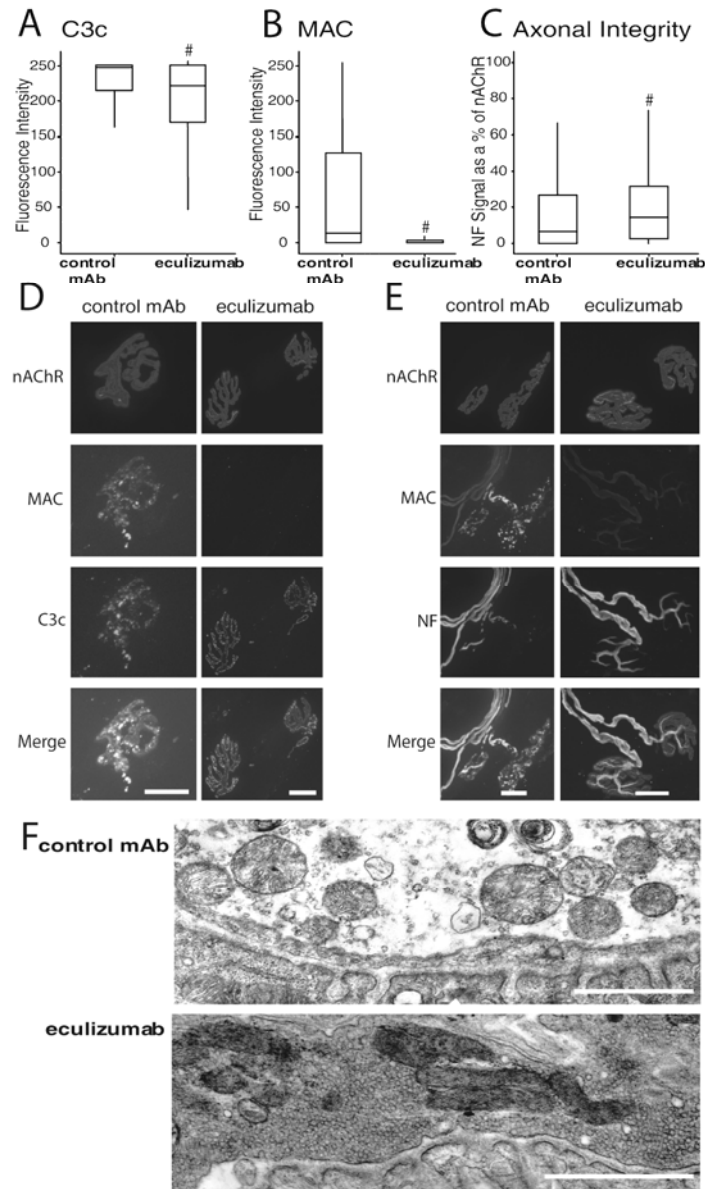


Figure 3.11. Morphological analysis of NMJs of diaphragm tissue from *in vivo* MFS mice. Mice were passively immunized with 1.5 mg anti-GQ1b ganglioside mAb, CGM3, followed 16 h later with concomitant injections of 0.5 ml 100% NHS (intraperitoneal) and eculizumab or control mAb (intravenous; 200 µg). **A-B.** C3c and membrane attack complex (MAC) deposition is reduced at neuromuscular junctions (NMJs) of eculizumab-treated mice compared with controls ($p < 0.01$). **C.** Neurofilament (NF) signal was significantly greater at NMJs of muscles from eculizumab-treated mice, compared with control ($p < 0.01$). **D-E.** Illustrative immunofluorescent images of NMJs in whole-mount muscle. Postsynaptic nicotinic acetylcholine receptors (nAChR) staining was used to delineate NMJs. **D.** C3c and MAC deposition. **E.** NF integrity and MAC deposition. **F.** Electron micrograph of eculizumab-protected nerve terminals with tightly packed synaptic vesicle and electron dense mitochondria with parallel cristae. At NMJs from control mAb-treated mice, nerve terminals are electron lucent with sparse synaptic vesicles and swollen mitochondria. $\#p < 0.01$, different from control mAb-treated. Scale bars in **D** and **E**: 20 µm; and in **F**: 1 µm.

Results

Eculizumab prevents complement-mediated structural and functional lesions in the *in vitro* MFS model

In the *in vitro* MFS model, treatment of diaphragm nerve-muscle preparations with CGM3 anti-GQ1b mAb and NHS, in the presence of an irrelevant isotype matched mAb (100 µg/ml), that served as a negative control for eculizumab, induced complement activation at NMJs. This was morphologically evidenced by C3c and MAC deposition (Figure 3.8A, B, D, E and F), as well as damaged pSCs and motor nerve terminals shown by EthD-1 staining and loss of neurofilament (NF) staining, respectively (Fig. 3.8C, E and F). These features were identical to those reported before (Goodyear et al., 1999; O'Hanlon et al., 2001; Halstead et al., 2004). The addition of 100 µg/ml eculizumab to the NHS as complement source completely prevented MAC deposition (Fig. 3.8B, D, E and F; $p < 0.001$) and terminal axonal NF loss (Fig. 3.8C and F; $p < 0.001$), while the deposition of the earlier complement component C3c was not affected (Figure 3.8A and D; $p = 0.12$). Furthermore, damage to pSCs was abolished as only 2% of the 1439 NMJs investigated had one or more EthD-1 positive nuclei, compared with 33% of 1529 NMJs investigated in control mAb-treated tissue (Figure 3.8E; $p < 0.001$).

These immunohistological observations paralleled the electrophysiological and functional observations. At CGM3 pre-incubated NMJs, NHS (40%) in the presence of the control mAb induced a large increase in the frequency of MEPPs, the postsynaptic events arising from spontaneous release of single acetylcholine quanta from the presynaptic motor nerve terminal, as previously observed (Goodyear et al., 1999). This effect was almost completely prevented by 100 µg/ml eculizumab. The MEPP frequency was about 0.7 s^{-1} before and after 50 µg/ml CGM3 incubation and rose to $34.0 \pm 4.6 \text{ s}^{-1}$ in the presence of NHS with 100 µg/ml control mAb added. In contrast the MEPP frequency was only $3.1 \pm 1.3 \text{ s}^{-1}$ in the presence of NHS with 100 µg/ml eculizumab added (Figure 3.9A and B; $n=5$ muscles; $p < 0.001$).

Eculizumab did not alter the muscle fibre resting membrane potential or MEPP amplitude, rise- and decay times (data not shown). As described before (Goodyear et al., 1999; Plomp et al., 1999), asynchronous twitching of individual muscle fibre occurs during NHS incubation (median visual score 4; $n=5$ muscles). Eculizumab prevented such high grade of twitching. Only a median score of 1 was observed (Figure 3.9C; $n=5$ muscles, $p < 0.01$, Mann-Whitney test), which equals the low basal levels observed in the observation periods before and after CGM3 incubation.

The final result of anti-CGM3/complement-mediated presynaptic damage is block of synaptic transmission at the NMJ due to the inability to release acetylcholine (Goodyear et al., 1999). Eculizumab completely prevented this effect. No "silent" NMJs (i.e. absence of MEPPs and nerve-stimulation evoked muscle action potentials) were encountered, whereas in the control mAb condition $19 \pm 2.6 \%$ of the total number of NMJs sampled were observed to be silenced (Figure 3.9D; $n=5$ muscles). Furthermore, we quantified the protective effect of eculizumab on muscle paralysis in the *in vitro* MFS model. Eculizumab inhibited loss of nerve stimulation-induced contraction force of hemi-diaphragm preparations in a concentration dependent manner following 200 µg/ml CGM3 and 33% NHS treatment (Figure 3.9E and F). In the control experiments without eculizumab, NHS induced almost complete loss of contraction force within 90 min. Addition of 3 or 6 µg/ml eculizumab to the NHS slowed down the rate of contraction force loss considerably (50% loss was observed

at 39 and 60 min, respectively, compared to 27 min in the control condition; Figure 3.9F). Higher eculizumab concentrations of 9 and 12 $\mu\text{g/ml}$ were almost completely protective (>90% of the initial contraction left after 90 min) while 25, 50 and 100 $\mu\text{g/ml}$ completely prevented any CGM3/NHS-induced loss of contraction. A Boltzmann sigmoidal curve fitted through the obtained concentration-effect data points yielded an EC_{50} of 7.1 $\mu\text{g/ml}$ for eculizumab under these conditions (Figure 3.9G). These immunohistological and functional analyses show that eculizumab efficiently prevents complement-mediated pathophysiological effects in the *in vitro* MFS model.

Eculizumab protects against neuropathy and respiratory paralysis in an *in vivo* MFS model

In order to determine the *in vivo* efficacy of eculizumab, we generated an *in vivo* MFS mouse model through intraperitoneal injection of CGM3 anti-GQ1b antibody and NHS as complement source. At 16 h after the CGM3 injection, a dose of 200 μg eculizumab or control mAb was administered systemically, via the tail vein, followed by intraperitoneal injection of 0.5 ml NHS. The protocol of different injection routes of eculizumab and NHS was applied to avoid the immediate inhibition of C5 in the NHS by eculizumab within the confinement of the peritoneal cavity. Mice treated with CGM3, NHS and control mAb ($n=10$) developed a general weak appearance, in some cases a low-back posture, invaginated abdominal flanks and breathing difficulties (panting) within 2 h following the NHS injection (see supplementary material). Intravenous eculizumab injection completely prevented the development of these symptoms ($n=11$). We quantified weakness with grip strength measurement in CGM3 pretreated mice, before and 2h after injection of control mAb or eculizumab and NHS (Figure 3.10A). Control group mice ($n=5$) pulled 56.0 ± 5.7 g just before the control mAb and NHS injection, while the eculizumab group mice ($n=5$) pulled 54.3 ± 8.4 g ($p=0.87$) at this stage. The pulling force 2 h after control mAb/NHS injection was 22% lower (43.7 ± 4.5 g; $p<0.005$). Eculizumab prevented such an effect (8% reduction; $p=0.07$). Respiratory disturbance was assessed with whole-body plethysmography continuously after mAb/NHS injection for a period of 6 h (Figure 3.10B and C; $n=5$ mice per group). The tidal volume before CGM3 injection was similar in both groups (0.21 ± 0.01 and 0.22 ± 0.03 ml in the control mAb and eculizumab group, respectively). A reduction of ~50% ($p<0.001$) was observed in the control mAb group at 4 and 6 h after NHS injection. Such a decrease was largely prevented by eculizumab (only 17% reduction at these time points, Figure 3.10B). Similarly, respiration rate was depressed in the control mAb group by ~30% ($p<0.01$) at 4 and 6 h post-NHS injection. In the eculizumab group, this reduction was only 7% (Figure 3.10C). Both treatment groups showed an equal initial reduction of about 40% of the respiration rate when measured 2 h post mAb/NHS, compared to the rate before CGM3 injection, which apparently was due to the intraperitoneal injection regimen. Example traces of the respiration flow rate obtained 4 h post-NHS are shown in Figure 3.10D.

We dissected hemi-diaphragm phrenic nerve preparations from *in vivo* CGM3/NHS treated mice at 4 h following NHS injection and performed electrophysiological measurements at NMJs, muscle contraction experiments, and detailed immunohistological analyses. Visual inspection indicated that only a very small part of the muscles from control mAb-treated mice contracted upon supramaximal electrical stimulation of the phrenic nerve, as compared to a complete contraction of muscles obtained from eculizumab-treated mice. In *in vitro* contraction experiments in

tissues harvested from passive immunizations, this effect was quantified (Figure 3.10E and F). Twitch and tetanic (40 Hz) tension was 0.07 ± 0.06 and 0.92 ± 0.61 g, respectively, in the control mAb group ($n=4$), while that in the eculizumab group ($n=4$) was 1.36 ± 0.29 and 9.26 ± 0.65 g, respectively, equalling the values of muscles from non-NHS treated age-matched mice (data not shown). With electrophysiological analysis we tested whether paralysis was caused by NMJ dysfunction. In dissected muscles from the control mAb group $66 \pm 7\%$ of the sampled NMJs had been “silenced”, i.e. there were no detectable MEPPs and no muscle action potentials upon nerve stimulations. In the eculizumab group only $3 \pm 2\%$ had been “silenced” (Figure 3.10G and H; $p<0.001$). Immunohistological analysis showed that CGM3 was deposited equally at NMJs of the two treatment groups (data not shown). C3c deposits were identified at NMJs of both groups, albeit with a somewhat less intensity in the eculizumab group (Figure 3.11A and D; $p<0.001$). MAC was clearly deposited at NMJs of muscles from control mAb-treated mice but virtually absent in the eculizumab-treated group (Figure 3.11B, D and E). Eculizumab prevented loss of terminal integrity at NMJs of CGM3- and NHS-treated mice, as evidenced by the NF signal intensity and pattern overlying the endplate region, i.e. terminal axonal branching clearly remaining intact (Figure 3.11C and E). In addition, electron microscopy showed the presence of a well-preserved presynaptic ultrastructure at the NMJ of eculizumab-treated mice in comparison with that of control mAb-treated mice which showed characteristic terminal swelling, synaptic vesicle depletion and swollen mitochondria (Figure 3.11G) (O'Hanlon et al., 2001). These electro-physiological, functional and immunohistological data show that complement-mediated terminal motor neuropathy occurs in our *in vivo* MFS model and that diaphragm paralysis contributes to the observed respiratory deficits. Most importantly, *in vivo* eculizumab treatment effectively prevented these *in vivo* neuropathological defects.

Discussion

Our previous *in vitro* studies demonstrated a key role for MAC, the pore-forming complement complex, consisting of C5b, C6, C7, C8 and C9 (Morgan, 1989), in mediating anti-ganglioside antibody-induced terminal motor neuropathy and pSC injury. We have observed a direct correlation between the extent of complement deposition, the degree of terminal axon injury, and the functional deficits at NMJs, suggesting a direct pathogenic action of complement in this model. In studies using C6-deficient NHS as a complement source (Halstead et al., 2004) or other means of preventing MAC formation (Halstead et al., 2005a), the development of morphological and electrophysiological lesions at NMJs is substantially attenuated, identifying MAC as the key factor. Similarly, in a rabbit model of anti-GM1 antibody-mediated acute motor axonal neuropathy, MAC formation is a prominent feature of the pathological phenotype suggesting a causal relationship between MAC formation and tissue injury (Susuki et al., 2007a). Whilst the contribution of MAC in mediating axonal injury in human inflammatory neuropathies cannot be readily assessed, it is evident from autopsy studies of GBS cases that MAC deposition at glial and axonal membranes is an important immunopathological factor (Hafer-Macko et al., 1996a; Putzu et al., 2000). Specific blockade of MAC may therefore be a way of preventing the pathological effects of the terminal complement while preserving the immunoprotective role of upstream complement components. Notwithstanding a

central role for complement activation with MAC formation in our MFS mouse model, it should be recognized that anti-ganglioside antibodies might exert complement independent effects on nerve function (Ortiz et al., 2001; Santafé et al., 2005; Buchwald et al., 2007; Lehmann et al., 2007). While such effects may be of relevance in certain pathophysiological circumstances, they are not evident in this model. Furthermore, antibodies found in GBS and related disorders are of the complement-fixing type (IgG1/3 and IgM; Willison and Veitch, 1994) and will inevitably activate complement.

Eculizumab is a humanized mAb directed against the complement protein C5 (Thomas et al., 1996). By binding to C5, eculizumab prevents the cleavage by C5-convertase into C5a and C5b, which is a crucial step in the terminal complement activation leading to MAC formation. Earlier components of the complement cascade are unaffected by C5 inactivation by eculizumab, such as the anaphylatoxin C3a which exerts potent proinflammatory effects, for example by mediating cellular chemotaxis. Eculizumab has recently undergone successful clinical trials in paroxysmal nocturnal haemoglobinuria, a disorder caused by complement-mediated lysis of red blood cells due to the genetic deficiency of complement inhibitory proteins (Hillmen et al., 2006; Hill et al., 2007). In the current study, eculizumab treatment was effective at ameliorating the clinical, electrophysiological and morphological symptoms of terminal motor neuropathy in experimental mouse MFS models, using anti-GQ1b mAb and NHS as complement source. Immunohistological analyses demonstrated virtually complete blockade of MAC formation at NMJs of eculizumab-treated mice and muscle-nerve preparations while C3c deposition remained almost unchanged.

In this study we have generated a new *in vivo* mouse model for MFS, displaying a respiratory paralysis phenotype that can be quantified with whole-body plethysmography that may prove useful in experimental drug studies. In this model it is likely that the almost complete paralysis of the diaphragm muscle is underlying the respiratory difficulties. The only slightly reduced grip strength of the MFS mice suggests that the respiratory paralysis is not accompanied by major limb muscle weakness. Normal contraction and NMJ function of dissected limb muscles support this idea (unpublished data, J.J. Plomp). This regional difference in paralysis is due to limited systemic distribution of the injected human complement from the peritoneal cavity rather than limited CGM3 distribution, as NMJs of dissected limb muscles have intense deposits of CGM3 and readily develop functional and morphological lesions when exposed to NHS (unpublished data, J.J. Plomp and S.K. Halstead).

One major difference between our mouse models and human MFS/GBS is the rapid time course at which the neuropathological symptoms develop, i.e. within tens of minutes in the *in vitro* model and within 2 h in the *in vivo* model, as compared with the days to weeks of onset of neuropathic symptoms in human patients. This could be due to the difference in the rate of anti-ganglioside antibody level elevation between the models and patients, i.e. a stepwise elevation by the incubation or injection occurring over seconds to minutes in the mouse models versus a slower, gradual increase in antibody production by B-cells in the patient occurring over days to weeks. The rapid onset of tissue injury in our *in vitro* and *in vivo* models required that eculizumab was added prior to the addition of NHS or injected concomitantly with NHS in order to protect against acute MAC mediated damage. This experimental protocol does not parallel the clinical context for MFS/GBS in which initiation of treatment would always follow (partial) symptom onset. Although eculizumab may not be expected to reverse existing MAC-mediated injury in patients, prompt

treatment would prevent further MAC deposition from taking place, hopefully limiting disease symptoms and thereby positively affecting the prognosis for long-term recovery (van Koningsveld et al., 2007).

Another, more fundamental, difference between our mouse MFS models and the human condition is the necessity to use human, i.e. heterologous, complement to induce the neuropathic lesions in mouse tissues. Previously, we attempted to generate an all-mouse model by intraperitoneal injection of anti-ganglioside antibody only (Goodyear et al., 1999). While we demonstrated antibody deposits overlying presynaptic nerve terminals, only sparse complement deposits were found in some mice and no functional defects were observed, even in mice lacking the complement regulators CD59a and DAF1 (unpublished data). However, mouse complement deposition at NMJs has been observed in such mice deficient in CD59a and/or DAF1 in a model of myasthenia gravis, an anti-acetylcholine receptor antibody-mediated neuromuscular disorder (Lin et al., 2002; Morgan et al., 2006; Kaminski et al., 2006). The reason for the apparent inability of complement fixing anti-ganglioside IgM or IgG mouse mAbs to lead to MAC deposition in our MFS model is unclear. It is most likely related to variations in complement activity and regulators in laboratory mice strains, as compared with humans. The complement activities of many different species have been compared in detail (Rice, 1950). In particular, a low haemolytic capacity of mouse serum seems due to the absence of classical pathway C5 convertase activity of mouse C4 (Ebanks and Isenman, 1996). For this reason, our studies have been pursued with NHS as a source of heterologous complement. Since eculizumab is specific for human C5 and unable to inhibit mouse C5 (Thomas et al., 1996), the data described here, despite being conducted in the mouse, relate very closely to human complement activation and inhibition. These results provide a basis for undertaking clinical trials with eculizumab in MFS and other neuropathies in which antibody-mediated complement activation is thought to be pathophysiologically relevant.

Supplementary material is available at *Brain* online